

# Decreased pulmonary vascular permeability in aquaporin-1-null humans

Landon S. King<sup>\*†‡§¶</sup>, Søren Nielsen<sup>||</sup>, Peter Agre<sup>†‡§</sup>, and Robert H. Brown<sup>\*†§\*\*††</sup>

<sup>\*</sup>Division of Pulmonary and Critical Care Medicine, Departments of <sup>†</sup>Medicine, <sup>‡</sup>Biological Chemistry, <sup>\*\*</sup>Anesthesiology and Critical Care Medicine, and <sup>††</sup>Radiology, <sup>§</sup>Johns Hopkins School of Medicine, Baltimore, MD 21287; and <sup>||</sup>Water and Salt Research Center, University of Aarhus, DK-8000 Aarhus, Denmark

Contributed by Peter Agre, November 21, 2001

The molecular determinants of water permeability in the human lung are incompletely defined. Aquaporins (AQP) are water-specific membrane channel proteins. AQP1 is present in endothelial cells in the lung, including those in the vascular plexus around the airways. Rare individuals have been identified who are deficient in AQP1. High-resolution computed tomography scans of the lung were used to evaluate the response to i.v. fluid challenge in two unrelated AQP1-null individuals and five normal controls. The airways and pulmonary vessels were measured at baseline and after i.v. administration of 3 liters of saline. Increases in airway wall thickness after fluid administration reflect peribronchiolar edema formation. Both control and AQP1 null subjects had approximately a 20% increase in pulmonary vessel area in response to saline infusion, suggesting similar degrees of volume loading. Control subjects had a 44% increase in the thickness of the airway wall, consistent with peribronchiolar edema formation. In marked contrast, airway wall thickness did not change in AQP1-null subjects in response to saline infusion. These studies indicate that AQP1 is a determinant of vascular permeability in the lung, and demonstrate a role for aquaporins in human pulmonary physiology.

Regulation of water movement between the vascular, interstitial, and airway compartments is critical for normal lung function. Disruption of this process contributes to alterations in gas exchange, lung mechanics, and local lung defense mechanisms. However, the molecular determinants of water transport in the respiratory tract remain incompletely defined, particularly for human pathophysiology.

Aquaporin-1 (AQP1), the archetypal membrane water channel protein, was initially described in red blood cells and renal proximal tubule epithelium (1). An extracellular epitope of AQP1 defines the Colton blood group antigen on red blood cells (2). Screening for anti-Colton antibodies by the International Blood Group Reference Laboratory identified only six Colton-null kindreds worldwide; a seventh individual has recently been described (3). Individuals in three of these kindreds were evaluated, and each was found to be homozygous for a different mutation in the *AQP1* gene with complete absence or marked reduction of AQP1 in red blood cell membranes (4). These individuals are unable to receive blood transfusions from normal donors, but otherwise reported no clinical symptoms as a consequence of AQP1 deficiency. Recent investigation of two AQP1-null individuals, however, revealed a decreased ability to concentrate urine maximally (5).

AQP1 is abundantly expressed in pulmonary vascular endothelium, particularly in endothelial cells of the vascular plexus around the airways (6). This distribution suggests a role for AQP1 in regulation of vascular water permeability in the lung. In the present study, we provide the first functional assessment of any aquaporin in human lung. By using high-resolution computed tomography (HRCT) to examine the response to fluid challenge, decreased pulmonary vascular permeability was demonstrated in two unrelated individuals with complete deficiency of AQP1.

## Methods

**Subjects.** The study was approved by our Institutional Review Board. Informed written consent was obtained from each sub-

ject. We evaluated two unrelated AQP1-null individuals and five normal controls (Table 1). None of the study subjects had underlying cardiac or pulmonary disease. With the exception of one AQP1-null individual (subject 2), all were nonsmokers. Subject 2 smoked less than one-half pack of cigarettes per week and had not smoked for one week before these studies.

**Study Design.** An 18-gauge i.v. catheter was placed in the dorsum of the hand or forearm. Baseline HRCT scans were acquired as described below. Subjects then received 1 liter of warmed normal saline solution during a 5-min period while supine in the computed tomography (CT) gantry, followed immediately by acquisition of another set of HRCT scans. This bolus/scan procedure was repeated two additional times in immediate succession to a total of 3 liters of i.v. saline and four HRCT scans.

**HRCT Image Acquisition.** Plethysmography was performed on each subject to determine the functional residual capacity and expiratory reserve volume (MedGraphics Body Plethysmography system; St. Paul, MN) with a constant-volume plethysmograph. These data were used to standardize the lung volume of each individual during HRCT scanning. Before each CT scan, subjects exhaled to residual volume, then inspired air delivered from a respiratory bag connected to the mouthpiece through a pneumatic valve. The fixed amount of air delivered from the bag was equal to the expiratory reserve volume determined by plethysmography, so that all scans were performed at functional residual capacity (residual volume + expiratory reserve volume) (7). Once all air was inspired from the respiratory bag, the pneumatic valve was closed so that constant lung volume was maintained for image acquisition.

All scans were acquired by using spiral CT (Somatom Plus 4; Siemens; Iselin, NJ) TIME/SCAN with settings of 140 kVp, 200 mA, 2-mm-slice thickness, rotation feed of 2 mm/s, and a reconstruction interval of 1 mm (total 53–61 scans per set). Scanner accuracy is measured weekly, and recalibrated if the measurement of water is off by more than 1%. The optimal spatial resolution of the scanner is 0.35 mm. Scanning began ≈5 cm above the anterior peak of the diaphragm at functional residual capacity, and moved caudally for a total of 5–6 cm. All analysis was performed on vessels and airways within this region of the lung. A reference scan was acquired before each spiral CT scan set to ensure reproducible positioning and image location in the lung. The images were reconstructed (16-bit 512 × 512 matrix; field of view of 200 mm) with a high-spatial frequency (resolution) algorithm that enhanced edge detection, at a window level of –450 Hounsfield units and a window width of 1,350 Hounsfield units. These window settings have been shown to allow optimal lung resolution (8). All airways visualized approx-

Abbreviations: AQP, aquaporin; CT, computed tomography; HRCT, high-resolution computed tomography.

<sup>†</sup>To whom reprint requests should be addressed. E-mail: lsking@welch.jhu.edu.

The publication costs of this article were defrayed in part by page charge payment. This article must therefore be hereby marked "advertisement" in accordance with 18 U.S.C. §1734 solely to indicate this fact.

**Table 1. Demographic and pulmonary function test characteristics of all subjects**

Subject	Age, yr	Sex	Ht, in	FEV <sub>1</sub> , liters	FVC, liters	FEV <sub>1</sub> /FVC, %	TLC, liters	VC, liters	FRC, liters	RV, liters
AQP1-null subjects										
1	37	F	63.5	2.81	3.26	86.4	4.58	3.45	1.89	1.13
2	57	F	67	3.38	4.21	80.5	6.43	4.2	3.67	2.23
Healthy subjects										
1	28	F	64	3.30	3.93	86.4	5.02	3.86	2.20	1.16
2	30	M	68	4.30	5.21	82.6	6.69	4.73	3.27	1.96
3	32	F	66	3.08	3.51	87.8	4.49	3.54	2.71	0.96
4	25	F	67	3.72	4.45	83.6	6.30	4.35	3.23	1.95
5	39	M	72	4.78	5.80	82.5	7.38	5.59	3.54	1.78

Ht, height (1 in = 2.54 cm); FEV<sub>1</sub>, forced expiratory volume in 1 sec; FVC, forced vital capacity; TLC, total lung capacity; VC, vital capacity; FRC, functional residual capacity; RV, residual volume.

imately perpendicular to the scan plane (long-to-short-axis ratio < 1.5:1) were measured. For repeated airway measurements in a given subject, adjacent anatomic landmarks, such as airway or vascular branching points, were defined on the control-state HRCT image. After each liter of i.v. fluid, the same airways in a given subject were matched with these adjacent parenchymal landmarks and measured.

**Analysis of Airways and Vessels.** The HRCT images were transferred as 16-bit data images to a UNIX-based workstation, and then analyzed with the airway analysis module of the VOLUMETRIC IMAGE AND DISPLAY ANALYSIS (VIDA) software package (Dept. of Radiology, Division of Physiologic Imaging, University of Iowa, Iowa City). To measure airway and vessel areas, the operator drew a rough estimate of the lumen isocontour within the airway or vessel. The software program then automatically located an isocontour of the airway lumen, or vessel outer perimeter, by sending out rays in a spoke-wheel fashion to a predesignated pixel intensity level that defines the luminal edge of the airway wall or outer edge of the vessel wall. The length of the rays was set at 6 pixels. The software program uses an algorithm for edge detection based on the “full-width-half-maximum” principle. The edge of the wall is defined by the program by the points along the rays where the pixel intensity changes to half its maximum through the wall. All full and partial pixels (full pixel size equals 0.23 mm<sup>2</sup> with our settings) within the adjusted isocontour were counted and represented the airway area. Accuracy and variability of the software program to measure known areas has been documented (9). Intra- and interobserver accuracy and variability of the software program with use of this HRCT technique in phantoms, consisting of rigid tubes of known areas, has been shown by us (10) and others (9) to be highly resistant to operator bias.

To measure airway wall thickness, the operator drew a line through the airway wall. The program automatically displayed a histogram of the pixel intensity along that line. The intensity points that represented the start of increased intensity associated with the airway wall between lumen and parenchymal background density were selected. The program then automatically measured the distance in pixels between the two points. The value for the airway wall thickness was converted to millimeters by multiplying by the pixel dimension in millimeters. Because the software we use is capable of measuring fractions of a pixel when the rays are drawn oblique to the side of a pixel, the measurements of wall thickness were not necessarily quantized to multiples of the pixel dimension. For the airways analyzed in this study, the airway walls ranged in thickness from 0.4 to 1.3 mm.

**Data Analysis.** For each subject, only airways and vessels that could be clearly visualized in all four scan sets were matched and measured. Airway luminal area, airway wall area, and

pulmonary vessel area are presented as a percent of the baseline value  $\pm$  SEM. These parameters were analyzed by using two-way ANOVA with Bonferroni/Dunn correction for multiple comparisons. Statistical significance was accepted at a two-tailed  $P \leq 0.05$ .

**Immunoelectron Microscopy.** Immunoelectron microscopy of human lung (surgical specimens) was performed as described (11). The specimen was fixed for 2 h in 4% paraformaldehyde and 0.1 M sodium cacodylate buffer (pH 7.2), infiltrated for 30 min with 2.3 M sucrose containing 2% paraformaldehyde, mounted on holders, and rapidly frozen in liquid N<sub>2</sub>. These blocks were used for cryosectioning or freeze-substitution with embedding in Lowicryl HM20. By using an automatic freeze substitution system (Reichert), samples were equilibrated sequentially for 3 days in 0.5% uranyl acetate in methanol at temperatures gradually increasing from  $-80^{\circ}\text{C}$  to  $-70^{\circ}\text{C}$ , and then rinsed in pure methanol for 24 h at  $-70^{\circ}\text{C}$  to  $-45^{\circ}\text{C}$ . At  $-45^{\circ}\text{C}$  the samples were serially infiltrated with Lowicryl HM 20 and methanol 1:1, 2:1, and finally pure HM20, before UV-polymerization for 2 days at  $-45^{\circ}\text{C}$  and 2 days at  $0^{\circ}\text{C}$ . Ultrathin Lowicryl sections (60–80 nm) or ultrathin cryosections (80 nm) were obtained with a Reichert Ultracut FSC ultracyromicrotome. The sections were incubated with affinity-purified anti-AQP1 antibodies (12) overnight, and labeling was visualized with goat-anti-rabbit IgG conjugated to 10-nm colloidal gold particles (GAR.EM10, BioCell Research Laboratories, Cardiff, U.K.). Control sections were incubated with antibody preadsorbed with purified AQP1 protein. The sections were stained with uranyl acetate for 10 min and examined in a Philips CM100 electron microscope (Philips Electronic Instruments, Mahwah, NJ).

## Results

The demographic and baseline pulmonary function data are presented in Table 1. The AQP1-null individuals were 37 and 57 years old. Subject 1 has a deletion of exon 1 of the *AQP1* gene, whereas subject 2 has a frameshift mutation (4); absence of AQP1 protein in these individuals was recently confirmed by protein immunoblot (5). Five healthy controls ranged in age from 28 to 40 years old. Baseline forced expiratory volume in 1 s was  $106 \pm 3\%$  of predicted for the healthy subjects, and  $111 \pm 11\%$  of predicted for the AQP1-null subjects ( $P = 0.46$ ). Baseline forced vital capacity was  $107 \pm 3\%$  and  $110 \pm 3\%$  of predicted for the control and AQP1-null subjects, respectively ( $P = 0.81$ ). None of the control or AQP1-null individuals had evidence of airway obstruction (Table 1).

We have shown that AQP1 is abundant in the endothelium of the vascular plexus around the airways in rat (6). Immunoelectron microscopy revealed a similar distribution for AQP1 in human lung, with abundant expression in both the apical and

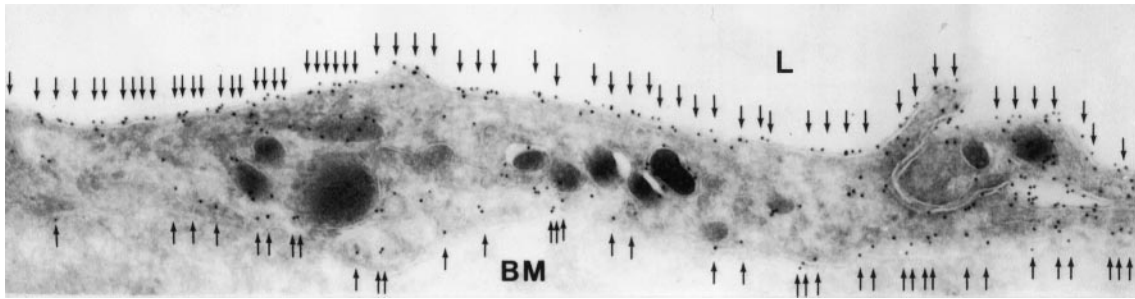


**Fig. 1.** Immunoelectron micrograph of endothelial cell from vascular plexus surrounding a bronchiole in human lung. Arrows indicate 10-nm immunogold particles labeling AQP1 on both the apical and basolateral membrane. L, lumen; BM, basement membrane. ( $\times 45,000$ )

basolateral membrane of capillary (Fig. 1) and venular endothelial cells (not shown).

The range of airways measured by HRCT was not different between the two groups—0.89–4.0 mm in diameter for the normal subjects and 0.89–3.6 mm in diameter for the AQP1-null subjects (15–33 airways measured per subject); the mean diameter was slightly smaller in the AQP1-null subjects ( $1.8 \pm 0.6$  mm vs. controls  $2.2 \pm 0.7$  mm;  $P < 0.01$ ). Airway wall area as a fraction of total airway area was not different between the two groups at baseline ( $P = 0.54$ ). The range of pulmonary vessels measured by HRCT was 1.2–4.6 mm in diameter for the normal subjects and 1.4–5.2 mm in diameter for the AQP1-null subjects (17–39 vessels measured per subject). At baseline, the mean pulmonary vessel diameter was not different between control subjects ( $2.4 \pm 0.05$  mm) and AQP1-null subjects ( $2.6 \pm 0.11$  mm) ( $P = 0.14$ ).

After infusion of 3 liters of saline, mean vessel area increased to  $121 \pm 2\%$  of baseline in control subjects (Figs. 2 and 3A) ( $P < 0.0001$  vs. baseline), and to  $124 \pm 3\%$  of baseline in AQP1-null subjects ( $P < 0.0001$  vs. baseline) (Fig. 3A). The magnitude of the vascular distention in response to fluid challenge was not different between the two groups ( $P = 0.10$ ).

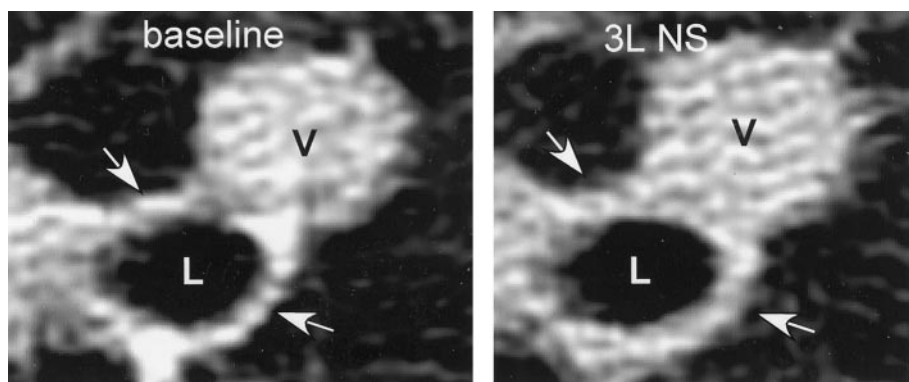
Volume loading with normal saline solution produced dramatically different effects on the airways of the control subjects compared with the airways of the AQP1-null subjects. All of the control individuals described mild chest tightness after saline infusion; neither of the AQP1-null individuals noted any change in symptoms. In control subjects, airway wall area increased after volume loading in a dose-dependent fashion to  $120 \pm 3\%$ ,  $131 \pm 4\%$ , and  $144 \pm 5\%$  of baseline, respectively, for 1, 2, and 3 liters of normal saline solution (Figs. 2 and 3B;  $P < 0.001$ ); similar increases in wall area were observed for all five control subjects. Wall area as a fraction of total airway area also increased after

fluid loading in the controls (not shown). In marked contrast, airway wall area did not change after fluid challenge in either of the AQP1 null subjects ( $P = 0.17$ ; Fig. 3B); wall area as a fraction of total airway area was also unchanged (not shown). Fluid challenge had no effect on the airway luminal area in either group ( $P = 0.10$ ).

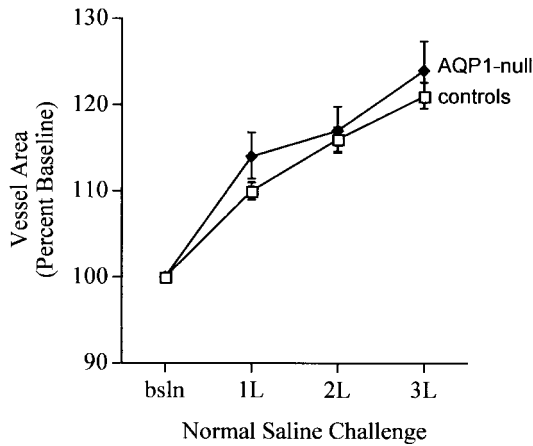
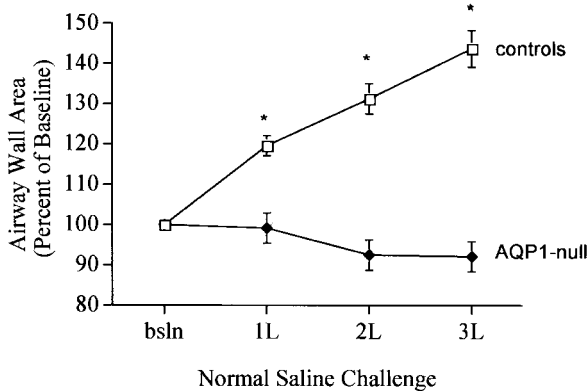
### Discussion

Aquaporins provide the molecular pathway for water transport in many tissues (13). Examples of aquaporin-related pathophysiology in humans are emerging. AQP2 is the vasopressin-responsive water channel protein in the collecting duct of the kidney (14); mutations in *AQP2* produce nephrogenic diabetes insipidus (15). Mutations in *AQP0* (MIP, major intrinsic protein of the lens) have been identified in some forms of congenital cataracts (16). In individuals with Sjögren's syndrome, AQP5 is not present in the apical membrane of acinar cells in the lacrimal glands (17) or salivary glands (18). Instead, AQP5 remains in the cytoplasm, the result of an apparent trafficking defect that likely contributes to the dry eyes and mouth that are the clinical hallmarks of that disorder. We recently reported that AQP1-null individuals have normal baseline renal function, but have a limited ability to maximally concentrate urine when water-deprived (5). In this report, we provide the first evidence of a role for AQP1 in determining vascular permeability in the human lung.

Several technical aspects of this study are critical to reliable interpretation of the results. First, performance of HRCT scans by using spiral CT in a single breath-hold at functional residual capacity minimized the potential contribution of changes in lung volume to airway characteristics (7). Second, the ability to match airways and vessels for measurement through serial scans has been extensively validated in both dog and human lung (7, 19,



**Fig. 2.** HRCT images of lung from a control subject at baseline and after i.v. administration of 3 liters of normal saline (3L NS). The vessel (V) dilated in response to fluid challenge. Airway luminal area (L) did not change after fluid challenge, but the airway wall thickened after saline administration (arrows).

**A****B**

**Fig. 3.** (A) Changes in pulmonary vessel area in control and AQP1-null subjects after fluid administration, expressed as percent of baseline area. ( $P > 0.05$  between groups;  $P < 0.001$  vs. baseline for both groups). (B) Changes in airway wall area after fluid challenge in AQP1-null and control subjects. Wall area is expressed as percent of baseline for each group. (controls,  $P < 0.0001$  vs. baseline; AQP1-null,  $P > 0.05$  vs. baseline;  $P < 0.0001$  between groups).

20). Third, although the mean airway size was slightly smaller in the AQP1-null group, the range of airways measured was similar in the two groups, and wall thickening in response to fluid challenge occurred in all airways independent of size in each control subject, consistent with previous observations in dog lung (19). Therefore, the dramatic difference in wall thickening in response to fluid challenge observed between the two groups is unlikely to be explained by subtle differences in airway size. Finally, by determining relative changes in wall thickness with the same airways through all scans, we minimized the potential complication of overestimating absolute distances as has been suggested for CT-based measurements (21).

The increase in airway wall thickness observed in the normal controls has not previously been reported in humans after fluid challenge (Figs. 2 and 3). This wall thickening most likely represents development of early peribronchial edema. Our findings are consistent with reports of peribronchial cuffing in humans with left ventricular failure (22), as well as classical descriptions of the early stages of pulmonary edema formation in animals (23). In marked contrast to the controls, saline infusion into AQP1-null individuals produced no change in airway wall thickness (Fig. 3).

Several points should be considered in assessing the differences in wall thickening observed in the two groups. Although

direct intrapulmonary hemodynamic monitoring could not be performed in our studies, pulmonary vascular distention measured by CT scan was found to correlate closely with both the volume load and the increase in pulmonary artery pressure in fluid-challenged dog lungs (19). Vascular distention measured by CT scan was identical in the control and AQP1-null subjects in this study, consistent with equivalent fluid loading. Additionally, the AQP1-null subjects had normal, not elevated, urine outputs in response to fluid loading in our study of their renal function (5), so they would not have eliminated the i.v. fluid more quickly than controls. We were unable to perform direct measurements of airway wall water in our subjects.

Could the increase in wall thickening that occurred over minutes represent something other than edema formation, for example vascular distention? In dogs, fluid challenge with i.v. saline produced vascular distention and airway wall thickening, whereas infusion of blood to achieve the same magnitude of vascular distention and increase in pulmonary artery pressure did not cause an increase in wall thickening (19). This result strongly suggests that vascular distention alone does not produce an increase in airway wall thickening. Airway wall thickening and edema formation have also been noted in sheep given bradykinin infusions into the bronchial circulation (24, 25), as well as in isolated dog lungs made grossly edematous by saline infusions into a sealed pulmonary vasculature (26). Taken together, we believe that our findings coupled with these considerations strongly predict that membrane water permeability was reduced in the AQP1-null group.

Fluid accumulation around the airways could result either from increased extravasation of fluid across the endothelium, or from decreased clearance of fluid from the interstitial space. Our findings are consistent with increased AQP1-mediated fluid extravasation from vessel to interstitium in the control individuals in this model of rapid fluid administration. However, fluid clearance from the peribronchiolar interstitial space to bronchial vessels has also been proposed in a variety of studies. Bland and colleagues demonstrated fluid clearance from the interstitial space around the airways during the perinatal period in rabbits (27). Jayr and Matthay demonstrated lung liquid clearance through the bronchial circulation in the absence of pulmonary blood flow in studies of adult sheep (28). Suggestions of both edema formation and edema clearance across this vascular bed are consistent with a role for AQP1 in transendothelial water flux, because *in vitro* studies have demonstrated that AQP1 can conduct water bidirectionally across cell membranes. In addition to potential contributions to the pathogenesis of pulmonary edema, AQP1 may participate in regulating the amount of interstitial fluid available to the overlying airway epithelium, and thereby contribute to generation or modulation of the airway surface liquid. This effect on permeability suggests roles for AQP1 in preservation of normal mucociliary transport, as well as in the pathophysiology of exercise- or cold-induced asthma, where changes in surface layer osmolality are thought to contribute to expression of the disease (29).

A central role for AQP1 in determining membrane osmotic water permeability is well established. In addition to studies in oocytes (30), mice with a deletion of the *Aqp1* gene had a 10-fold reduction in the osmotic water permeability of the pulmonary vascular bed compared with wild-type mice, as well as a 2-fold reduction in permeability after an increase in pulmonary hydrostatic pressure (31). The observation that acute edema formation was not different between *Aqp1*-null and wild-type mice in response to inflammatory stimuli (32) suggests both compensation and redundancy in the systems for water homeostasis in the lung. Perhaps more importantly, potential distinctions between mechanisms regulating basal water homeostasis from those contributing to edema formation or resolution are not well understood. It remains unclear whether AQP1 facilitates water

transport in all of those conditions or only in select circumstances. Additionally, differences between humans (5) and mice (33, 34) in the renal manifestations of AQP1 deficiency, as well as recent observations of species differences in AQP distribution in lung epithelium (35, 36) suggest potential limitations in our ability to extrapolate from animal models.

Our observations in rare AQP1-null humans provide the first evidence of a role for AQP1 in determining vascular water permeability in human lung. On the basis of the extremely low frequency of the genotype, and our observations of renal function in these individuals (5), we believe it is likely they have some form of compensation for AQP1 deficiency. Future investigation may provide insight into the potential contribution of acquired

changes in AQP1 expression or function to lung water homeostasis in a variety of pathophysiologic conditions.

We thank Beatrice Mudge and the Pulmonary Function Laboratory of the Johns Hopkins Hospital for technical assistance with these studies, and Richard H. Boucher and John H. Newman for critical evaluation of the manuscript. This study was supported by the National Institutes of Health's Heart, Lung, and Blood Institute (L.K., P.A., and R.B.); the Cystic Fibrosis Foundation (L.K. and P.A.); the Johns Hopkins University School of Medicine General Clinical Research Center, National Institutes of Health/National Center for Research Resources Grant M01 RR00052; the European Commission (KA 3.1.2 and 3.1.3); and the Karen Elise Jensen Foundation (S.N.). The Water and Salt Research Center was established and supported by the Danish National Research Foundation (S.N.).

1. Denker, B. M., Smith, B. L., Kuhajda, F. P. & Agre, P. (1988) *J. Biol. Chem.* **263**, 15634–15642.
2. Smith, B. L., Preston, G. M., Spring, F. A., Anstee, D. J. & Agre, P. (1994) *J. Clin. Invest.* **94**, 1043–1049.
3. Joshi, S. R., Wagner, F. F., Vasantha, K., Panjwani, S. R. & Flegel, W. A. (2001) *Immunohematology* **41**, 1273–1278.
4. Preston, G. M., Smith, B. L., Zeidel, M. L., Moulds, J. J. & Agre, P. (1994) *Science* **265**, 1585–1587.
5. King, L. S., Choi, M., Fernandez, P. C., Cartron, J. P. & Agre, P. (2001) *N. Engl. J. Med.* **345**, 175–179.
6. King, L. S., Nielsen, S. & Agre, P. (1996) *J. Clin. Invest.* **97**, 2183–2191.
7. Brown, R. H., Croisille, P., Mudge, B., Diemer, F., Permutt, S. & Toggias, A. (2000) *Am. J. Respir. Crit. Care Med.* **161**, 1256–1263.
8. Webb, W. R., Gamsu, G., Wall, S. D., Cann, C. E. & Proctor, E. (1984) *Invest. Radiol.* **19**, 394–398.
9. Amirav, I., Kramer, S. S., Grunstein, M. M. & Hoffman, E. A. (1993) *J. Appl. Physiol.* **75**, 2239–2250.
10. Herold, C. J., Brown, R. H., Mitzner, W., Links, J. M., Hirshman, C. A. & Zerhouni, E. A. (1991) *Radiology* **181**, 369–374.
11. Nielsen, S., King, L. S., Christensen, B. M. & Agre, P. (1997) *Am. J. Physiol.* **273**, C1549–C1561.
12. Smith, B. L. & Agre, P. (1991) *J. Biol. Chem.* **266**, 6407–6415.
13. King, L. S., Yasui, M. & Agre, P. (2000) *Mol. Med. Today* **6**, 60–65.
14. Knepper, M. A., Wade, J. B., Terris, J., Ecelbarger, C. A., Marples, D., Mandon, B., Chou, C-L., Kishore, B. K. & Nielsen, S. (1996) *Kidney Int.* **49**, 1712–1717.
15. Deen, P. M., Verdijk, M. A., Knoers, N. V., Wieringa, B., Monnens, L. A., Van Os, C. H. & Van Oost, B. A. (1994) *Science* **264**, 92–95.
16. Berry, V., Francis, P., Kaushal, S., Moore, A. & Bhattacharya, S. (2000) *Nat. Genet.* **25**, 15–17.
17. Tsubota, K., Hirai, S., King, L. S., Agre, P. & Ishida, N. (2001) *Lancet* **357**, 688–689.
18. Steinfeld, S., Cogan, E., King, L. S., Agre, P., Kiss, R. & Delporte, C. (2001) *Lab. Invest.* **81**, 143–148.
19. Brown, R. H., Zerhouni, E. A. & Mitzner, W. (1995) *J. Appl. Physiol.* **78**, 1070–1078.
20. Brown, R. H., Zerhouni, E. A. & Mitzner, W. (1995) *J. Appl. Physiol.* **79**, 1242–1248.
21. Wood, S. A., Zerhouni, E. A., Hoford, J. D., Hoffman, E. A. & Mitzner, W. (1995) *J. Appl. Physiol.* **79**, 1687–1697.
22. Don, C. & Johnson, R. (1977) *Radiology* **125**, 577–582.
23. Staub, N. C., Nagano, H. & Pearce, M. L. (1967) *J. Appl. Physiol.* **22**, 227–240.
24. Brown, R. H., Mitzner, W. & Wagner, E. M. (1997) *J. Appl. Physiol.* **83**, 366–370.
25. Brown, R. H., Mitzner, W., Bulut, Y. & Wagner, E. M. (1997) *J. Appl. Physiol.* **82**, 491–499.
26. Forster, B. B., Muller, N. L., Mayo, J. R., Okazawa, M. & Wiggs, B. J., Pare, P. D. (1992) *Chest* **101**, 434–437.
27. Bland, R. D., McMillan, D. D., Bressack, M. A. & Dong, L. (1980) *J. Appl. Physiol.* **49**, 171–177.
28. Jayr, C. & Matthay, M. A. (1991) *J. Appl. Physiol.* **71**, 1679–1687.
29. Anderson, S. D. & Toggias, A. G. (1995) in *Asthma and Rhinitis*, eds. Busse, W. W. & Holgate, S. T. (Blackwell Scientific, Oxford), pp. 1178–1195.
30. Preston, G. M., Carroll, T. P., Guggino, W. B. & Agre, P. (1992) *Science* **256**, 385–387.
31. Bai, C., Fukuda, N., Song, Y., Ma, T., Matthay, M. A. & Verkman, A. S. (2000) *J. Clin. Invest.* **103**, 555–561.
32. Song, Y., Fukuda, N., Bai, C., Ma, T., Matthay, M. A. & Verkman, A. S. (2000) *J. Physiol.* **525**, 771–779.
33. Ma, T., Yang, B., Gillespie, A., Carlson, E. J., Epstein, C. J. & Verkman, A. S. (1998) *J. Biol. Chem.* **273**, 4296–4299.
34. Schnermann, J., Chou, C-L., Ma, T., Traynor, T., Knepper, M. A. & Verkman, A. S. (1998) *Proc. Natl. Acad. Sci. USA* **95**, 9660–9664.
35. Kreda, S. M., Gynn, M. C., Fenstermacher, D. A., Boucher, R. C. & Gabriel, S. E. (2001) *Am. J. Respir. Cell Mol. Biol.* **24**, 224–234.
36. King, L. S. & Agre, P. (2001) *Am. J. Respir. Crit. Care Med.* **24**, 221–223.